

An on-line multi-parameter analyzing optical biosensor for real-time and non-invasive monitoring of plant stress responses *in vivo*

ZHANG LingRui, XING Da[†] & WEN Feng

MOE Key Laboratory of Laser Life Science & Institute of Laser Life Science, South China Normal University, Guangzhou 510631, China

Photosynthetic dysfunction and reactive oxygen species (ROS) production are the common features of plant stress responses. Based on quantitative measurement of ROS production and delayed fluorescence (DF) emission, which is an excellent marker for evaluating photosynthesis, an on-line multi-parameter analyzing optical biosensor for detecting plant stress responses was developed. Performances of the proposed biosensor were tested in the wild type (WT) *Arabidopsis* and heat shock protein (Hsp) 101 T-DNA knockout mutant (*hsp101*) plants with different thermotolerance. Results demonstrated that DF intensity correlates with net photosynthesis rate (Pn) in response to elevated temperature in both the WT *Arabidopsis* and *hsp101* mutant plants. The light response characteristics and the recovery dynamics of the DF intensity were also in line with those of Pn in both the WT *Arabidopsis* and *hsp101* mutant plants after heat stress (HS, 40°C for 30 min), respectively. In all experiments discussed above, the *hsp101* plant showed the worse photosynthetic performance than the WT plant. Moreover, after HS, more ROS production in the *hsp101* mutant than in WT *Arabidopsis*, which was found to be mainly localized at chloroplasts, could be directly detected by using the proposed biosensor. In addition, the *hsp101* mutant showed severer chloroplasts alterations than the WT plant within the first 1 h of recovery following HS. Nevertheless, pre-infiltration with catalase (CAT) reduced ROS production and prevented the declines of the DF intensity. Therefore, HS-caused declines of photosynthetic performance might be due to oxidative damage to photosynthetic organelle. To sum up, we conclude that Hsp101 plays an important role in preventing oxidative stress, and the proposed optical biosensor might be a powerful tool to determine plant stress responses and identify plant resistant difference.

heat stress, heat shock protein 101, reactive oxygen species, delayed fluorescence, net photosynthesis rate

Temperature is a major environmental factor that affects plant growth and productivity. Traditional examination of plant responses to increased temperature and identification of high temperature resistant species are carried out by means of biochemical assays such as detection of chlorophyll breakdown products, determination of membrane ion leakage and analysis of heat shock proteins (Hsp) expression. Apparently, the sample preparation procedure of these methods is rather complicated and time-consuming. At present, gas exchange and chlorophyll fluorescence techniques are the main approaches

for detecting plant stress responses *in vivo*^[1]; however, gas exchange technique is prone to interference from environmental factors^[2]. Although chlorophyll fluorescence technique is a fast method for studying plant physiology as well as the interaction between plants and environmental factors, some difficulties have been enco-

Received June 11, 2008; accepted October 24, 2008

doi: 10.1007/s11434-009-0157-8

[†]Corresponding author (email: xingda@scnu.edu.cn)

Supported by the National Natural Science Foundation of China (Grant No. 30870676), National High-Tech Research & Development Program of China (Grant No. 2007AA10Z204) and Key Project of Science Research of South China Normal University (Grant No. 08GDKC03)

untended^[1,2].

It has long been known that photosynthetic apparatus is one of the most heat-sensitive aspects and it can be damaged by heat stress (HS) before other stress symptoms could be detected^[3]. The pronounced sensitivity of photosynthesis towards HS can make photosynthesis be used as an HS indicator to early detect disturbances and damage in plant tissue^[4]. Under HS condition, dysfunction of photosynthetic processes and alterations of chloroplasts structure have been attributed to oxidative damages because producing large amounts of ROS is an inevitable consequence in chloroplasts when plants encounter high temperature^[5,6]. Among the key processes of photosynthesis, the rate of photosystem (PS) II electron transport in plants is strongly linked to net photosynthesis rate (Pn) and is the sensitive target of oxidative damages caused by HS^[7,8]. Inhibition of photosynthesis by HS can be attributed to an impairment of electron transport activity^[9,10]. Therefore, the effects of HS on photosynthesis can be ascertained by directly detecting the changes in the capacity of PSII electron transport.

Delayed fluorescence (DF) of chloroplast emits from PSII through inverse photochemistry reactions. The mechanism of DF generation has been described in greater detail elsewhere^[2,11–14]. DF has many practical applications^[12]. It can be used as a sensitive indicator to detect herbicides toxicity and acid rain pollution as well as to ascertain plant senescence process *in vivo*, providing more valuable information about photosynthetic processes than chlorophyll fluorescence^[12–15]. Investigation of DF invokes particular interest because its intensity depends directly on the rate of backward electron transport reactions in the reaction centre of PSII. In its turn backward electron transport reactions are determined by quantum efficiency of primary processes of photosynthesis^[2]. It has been documented that when photorespiration is suppressed, there is a good correlation between the quantum efficiencies of PS and the efficiency of CO₂ fixation^[16]. More recently, a lot of contrastive experiments further have demonstrated that DF intensity also correlates with Pn in many plant species even under field conditions^[2]. Accordingly, the analysis of DF behaviour can be useful in assessing the state of the photosynthetic processes^[12–15].

In this paper, an on-line multi-parameter analyzing optical biosensor for real-time and non-invasive monitoring of plant stress responses *in vivo* was developed. The proposed optical biosensor, which was equipped

with two kinds of light-emitting diode (LED) lattices with different emission peaks as excitation light source and a compact single photon counting module (SPCM) to collect DF and other fluorescence signals, is portable and can evaluate plant stress responses *in vivo*. The applicability of the proposed biosensor for detecting HS responses was investigated in the wild type (WT) *Arabidopsis* and Hsp101 T-DNA knockout mutant (*hsp101*) plants with different thermotolerance. Results demonstrated that DF intensity correlates with Pn in each *Arabidopsis* after HS, and this biosensor can rapidly determine plant stress responses and accurately identify the differences in thermotolerance.

1 Materials and methods

1.1 Materials

The *Arabidopsis* (*Arabidopsis thaliana*) Col-0 (WT) and Col-0 *Hsp101* (At1g74310) T-DNA insertion homozygous line SALK_066374 (*hsp101*) were grown in soil culture in a plant growth chamber (Conviron, model E7/2, Canada) with a 16 h light photoperiod (100 $\mu\text{mol photons m}^{-2} \cdot \text{s}^{-1}$) and a relative humidity of 75%/80% (light/dark) at 23°C/21°C (light/dark). 2', 7'-dichlorodihydrofluorescein diacetate (H₂DCFDA) and catalase (CAT) were obtained from Molecular Probes (Eugene, OR, USA) and Sigma-Aldrich China (Shanghai, China), respectively.

1.2 Isolation of *Arabidopsis* protoplasts

The isolation of protoplasts from the WT and *hsp101* mutant plants (14–21 d old) was carried out at room temperature, according to a modified procedure as described previously^[17].

1.3 HS treatment

The attached leaves or protoplasts of the WT and *hsp101* mutant plants were heated in water bath at 40°C for 30 min as HS treatment, which had been demonstrated to induce a significant increase in the level of Hsp101 when compared with normal conditions (26°C, 30 min) in WT *Arabidopsis*^[18,19], and then allowed to recover for indicated time at their own optimum temperatures of photosynthesis (the WT *Arabidopsis* at 26°C and the *hsp101* mutants at 20°C).

1.4 Laser confocal scanning microscopy (LCSM) and imaging organelle *in vivo*

Microscopic observations were performed using a Zeiss

LSM 510 laser confocal scanning microscope (LSM510/ConfoCor2, Carl-Zeiss, Jena, Germany). H₂DCFDA signals were visualized with excitation at 488 nm from an Ar-Ion laser and emission at 500–550 nm using a band pass filter. Chloroplast autofluorescence (488 nm excitation) was visualized at 650 nm with a long pass filter. For three-dimensional (3D) reconstructions, optical sections of cell were taken, and Z series were performed with 0.5 μm steps. All images were taken with the 100 \times oil-immersion objectives on the Zeiss LSM 510 and analyzed with Zeiss Rel3.2 image processing software (Zeiss, Germany).

1.5 Pn measurement

At the indicated recovery time point, Pn of the leaves of the WT and *hsp101* mutant plants was measured using a commercially available system (LI-6400; LI-COR, Inc., USA) equipped with a 6400-15 *Arabidopsis* Chamber (1.0 cm in diameter) and artificial illumination. Irradiation intensity was saturated (250 $\mu\text{mol photons m}^{-2} \cdot \text{s}^{-1}$ for the WT *Arabidopsis* and 150 $\mu\text{mol photons m}^{-2} \cdot \text{s}^{-1}$ for the *hsp101* mutants). Supply of CO₂ (400 ppm) to the leaves was controlled by a built-in CO₂ injection system.

1.6 On-line multi-parameter analyzing optical biosensor and DF measurement *in vivo*

DF emission from samples after irradiation was recorded with a custom-built on-line multi-parameter analyzing optical biosensor. The technical details of this biosensor were described elsewhere^[2]. Here some improvements and a brief summary of measurement process will be presented (Figure 1). The irradiation source of the biosensor has been improved and consists of two sets of LEDs, including red LED ($\lambda = 628 \text{ nm}$, half wave width = 10 nm, single duct output luminous flux = 20 Lm) and blue LED ($\lambda = 470 \text{ nm}$, half wave width = 10 nm, single duct output luminous flux = 20 Lm). Three red LEDs and three blue LEDs were alternately and uniformly arrayed along a circumference for homogeneous irradiation of the leaves. The irradiance intensities of red LEDs and blue LEDs were adjusted by changing the current. After Pn measurement, the leaves of the WT and *hsp101* mutant plants were placed inside the chambers of the biosensor to dark-adapt for 5 min before the irradiation source was turned on. For DF measurements *in vivo*, the leaves were irradiated by red LED for 0.2 s. The light intensity was the same as in Pn measurement.

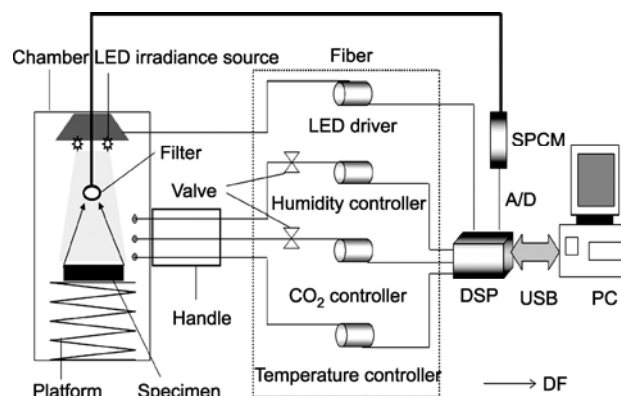


Figure 1 A diagram of the on-line multi-parameter analyzing optical biosensor: LED, SPCM, and DSP represent the light-emitting diode, single photon counting module, and digital signal processor, respectively.

The DF emission was collected at 0.26 s upon the completion of the light irradiation by an optical fiber bundle after passing a 650 nm long pass filter and transmitted to an SPCM (MP963, Perkin-Elmer, Wiesbaden, Germany) with a wavelength detection range of 185–850 nm. The output signals were further processed by a digital signal processor (DSP, TMS320C6416) (local control mode) or a computer (remote control mode). The DF intensity was obtained by the integration between 0.26 and 5.26 s in the DF decay dynamics curve and registered as count per second (cps). All measurements were performed in dark.

1.7 ROS detection

ROS production in protoplasts or leaves was determined by detecting the fluorescence of DCF, the product of oxidation of H₂DCFDA, as described previously^[17]. At the indicated recovery time point, the *Arabidopsis* protoplasts or leaves were incubated with H₂DCFDA at a final concentration of 5 $\mu\text{mol/L}$ for 10 min in dark. The intracellular ROS production and distribution were visualized under the Zeiss LSM 510. The fluorescence of DCF in leaves was quantified with the custom-made optical biosensor in dark, with an excitation wavelength of 470 nm from the blue LEDs and emission wavelengths between 500 and 550 nm using a band pass filter.

2 Results

2.1 The responses of DF intensity and Pn to different temperatures

To test the accuracy of the proposed optical biosensor, we first compared DF intensity with Pn in response to

elevated temperature in the WT and *hsp101* mutant plants. As shown in Figure 2, at 2 h following the indicated temperature treatment for 30 min, the DF intensity responded to elevated temperature in a manner consistent with Pn in the WT and *hsp101* mutant plants, respectively. Measurements of the DF intensity and Pn both showed that the optimum temperatures of photosynthetic performance for the WT *Arabidopsis* and *hsp101* mutant plants differed by about 6°C. For the *hsp101* mutant, the DF intensity and Pn were both inhibited by temperatures higher than about 20°C, whereas for the WT *Arabidopsis* inhibition occurred at temperatures higher than 26°C (Figure 2). DF intensity and Pn in the WT *Arabidopsis* were inhibited by approximately 36.1% and 32.2% at 40°C compared with 26°C, respectively, whereas DF intensity and Pn in the *hsp101* mu-

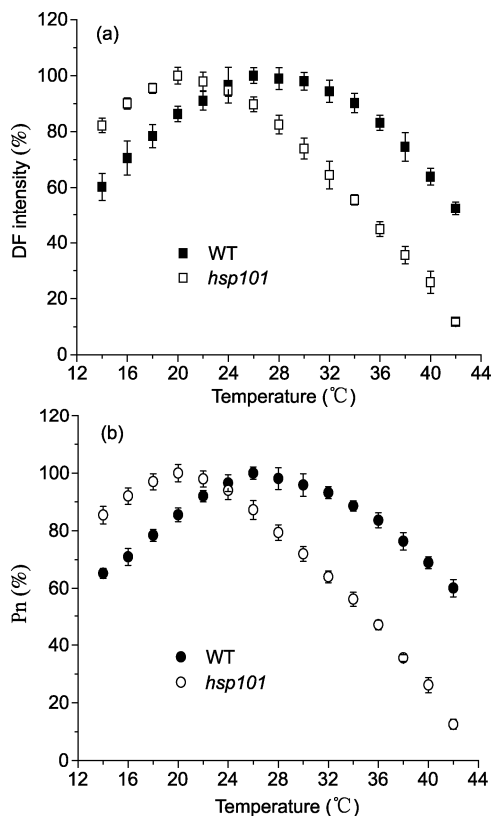


Figure 2 The responses of DF intensity and Pn to evaluated temperatures in the WT and *hsp101* mutant plants. The data for DF intensity (a) are expressed as a percentage of the intensity measured at the optimum temperature; $(21.75 \pm 1.37) \times 10^4$ and $(18.4 \pm 0.87) \times 10^4$ cps for the WT *Arabidopsis* at 26°C and the *hsp101* mutant at 20°C, respectively. The data for Pn (b) are expressed as a percentage of the rate measured at the optimum temperature; 21.74 ± 1.32 and $19.1 \pm 0.96 \mu\text{mol CO}_2 \text{ m}^{-2} \cdot \text{s}^{-1}$ for the WT *Arabidopsis* at 26°C and the *hsp101* mutant at 20°C, respectively. Data are the mean values of five replicates; SEs are shown when larger than the symbol.

tant were inhibited by approximately 74.1% and 73.9% at 40°C compared with 20°C, respectively (Figure 2), suggesting the inhibitory extent of the DF intensity was similar to that of Pn in the two plants, respectively.

2.2 The responses of DF intensity and Pn to irradiance intensity after HS

Next, the characteristics of light responsiveness of DF intensity and Pn were contrastively analyzed in the WT and *hsp101* mutant plants after HS, respectively. It was clear that DF intensity and Pn responded to excitation intensity in a similar manner in each *Arabidopsis* at 2 h following HS (Figure 3). At any given excitation intensity, DF intensity and Pn were higher in the WT *Arabidopsis* than in the *hsp101* mutant after HS, respectively (Figure 3(a) and (b)). As excitation intensity increased, both DF intensity and Pn initially increased linearly, then reached a plateau at the same excitation intensity and leveled off at the same time with a further rise in excitation intensity in each *Arabidopsis*, respectively

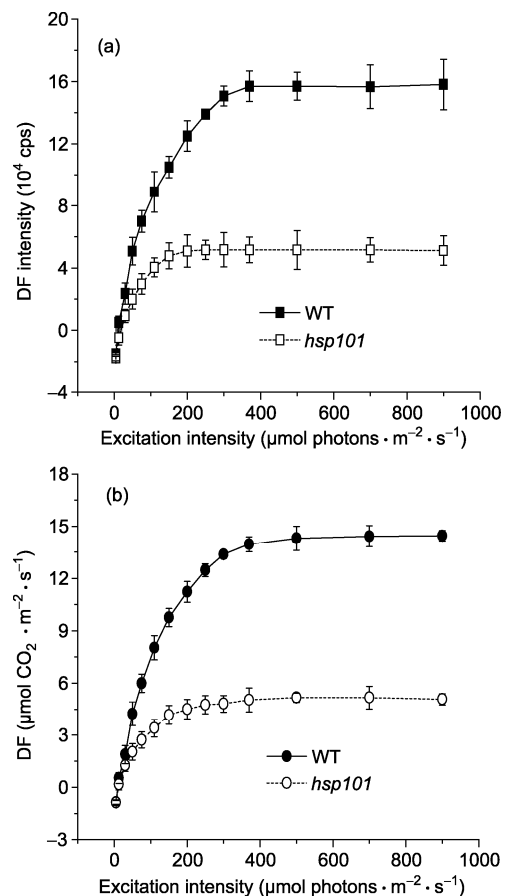


Figure 3 The responses of DF intensity (a) and Pn (b) to excitation intensity in the WT *Arabidopsis* and *hsp101* mutant plants after 2 h of recovery following HS. Data are the mean values of five replicates; SEs are shown when larger than the symbol.

(Figure 3). For example, DF intensity and Pn were saturated at the same excitation intensity of $250 \mu\text{mol photons m}^{-2} \cdot \text{s}^{-1}$ in the WT *Arabidopsis*. However, DF intensity and Pn were saturated at the same excitation intensity of $150 \mu\text{mol photons m}^{-2} \cdot \text{s}^{-1}$ in the *hsp101* mutant (Figures 3(a) and (b)). Moreover, the light saturation curve was the same for the inverse light changes (from high to low light intensity) (data not shown).

2.3 Recovery dynamics of DF intensity and Pn after HS

The recovery dynamics of DF intensity and Pn were also further investigated in the two plants after HS. As shown in Figure 4, after 2 h of recovery following HS, both DF intensity and Pn declined to the lowest level in the two plants. Subsequently, DF intensity and Pn consistently recovered to the level of control after cooling the attached leaves from HS for 10 h in the WT *Arabidopsis*

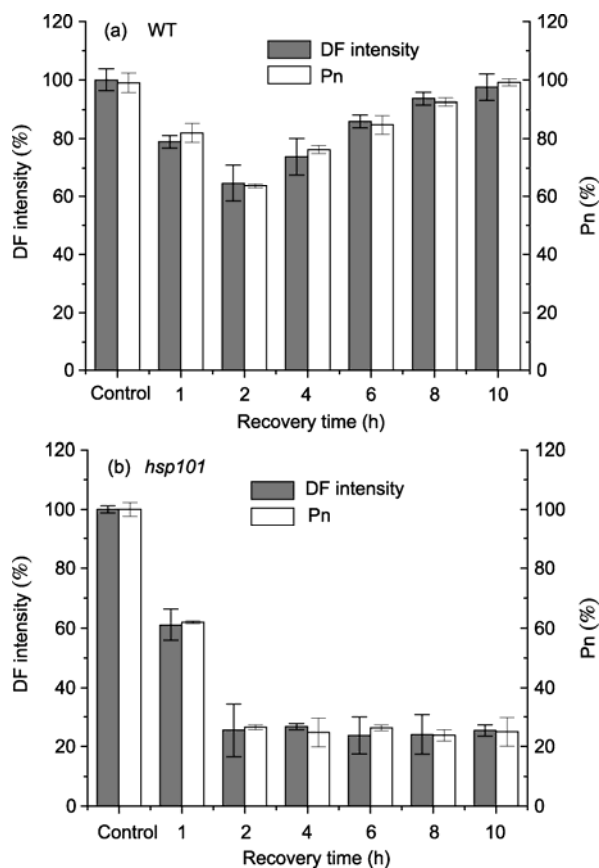


Figure 4 The recovery dynamics of DF intensity and Pn in the WT *Arabidopsis* and *hsp101* mutant plants after cooling from high temperature. (a) DF intensity and Pn in the WT *Arabidopsis* recovered from HS were measured after cooling the seedlings to 26°C . (b) DF intensity and Pn in the *hsp101* mutant recovered from HS were measured after cooling the seedlings to 20°C . Data are the mean values of five replicates; SEs are shown when larger than the symbol.

but not in the *hsp101* mutant plants (Figure 4(a) and (b)). This implied that HS caused irreversible damage to the photosynthetic apparatus of the *hsp101* mutant. But the damage to the photosynthetic apparatus caused by the same HS could reversibly recover in the WT *Arabidopsis*.

2.4 ROS Production after HS and effects of antioxidant on DF intensity

Considering that ROS production is a common feature in response to environmental stress^[5], we therefore examined the levels of ROS in the WT *Arabidopsis* and *hsp101* mutant plants after HS by using the proposed optical biosensor. Compared with the control, a 5- and 7-fold increase in DCF fluorescence could be observed in the WT *Arabidopsis* and *hsp101* mutant plants after 30 min of recovery following HS, respectively (Figure 5(a)). Pre-infiltrating the leaves with CAT, an H_2O_2 -specific scavenger, arrested the increases in DCF fluo-

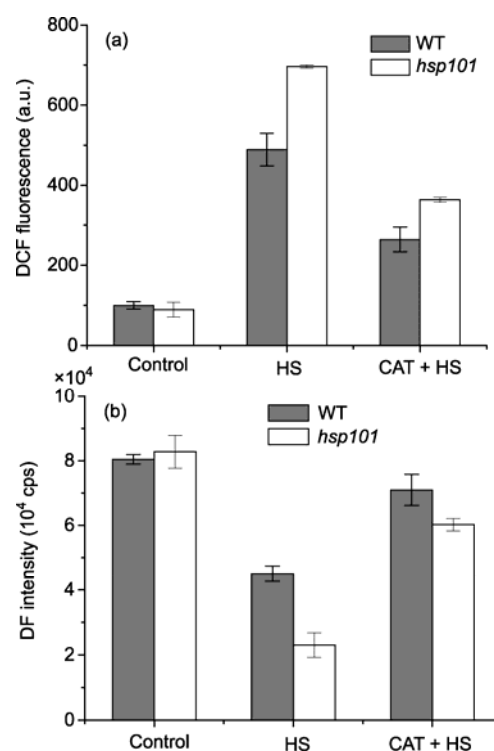


Figure 5 ROS production after HS and effects of antioxidants on ROS production and DF intensity. (a) The leaves were pre-incubated without or with CAT at $100 \text{ U} \cdot \text{mL}^{-1}$ final concentration for 30 min in dark and then treated with HS. At 30 min of recovery following HS, the samples were subjected to $5 \mu\text{mol/L}$ H_2DCFDA for 10 min in dark, and the concentration of H_2O_2 was measured by the optical biosensor as described in "Materials and methods". (b) After 2 h of recovery following HS, DF intensity in samples was measured by the optical biosensor as described in "Materials and methods". Data are the mean \pm SEs of five replicates.

rescence induced by HS in the two plants. Intriguingly, the declines in DF intensity could also be prevented by infiltrating the leaves with CAT in the two plants (Figure 5(b)).

2.5 Subcellular localization of ROS and changes in chloroplasts morphology after HS

The protection of leaves against the decline in DF intensity by antioxidants posed the question as to how and where ROS are produced in living cells (Figure 5(b)). To address these questions and to verify the new function of the optical biosensor for measuring DCF fluorescence, we used an LCSM to monitor intracellular ROS production and to visualize the photosynthetic apparatus at the single cell level *in vivo*. Compared with the control, large DCF-stained regions were found to be mainly localized at chloroplasts in the WT *Arabidopsis* and

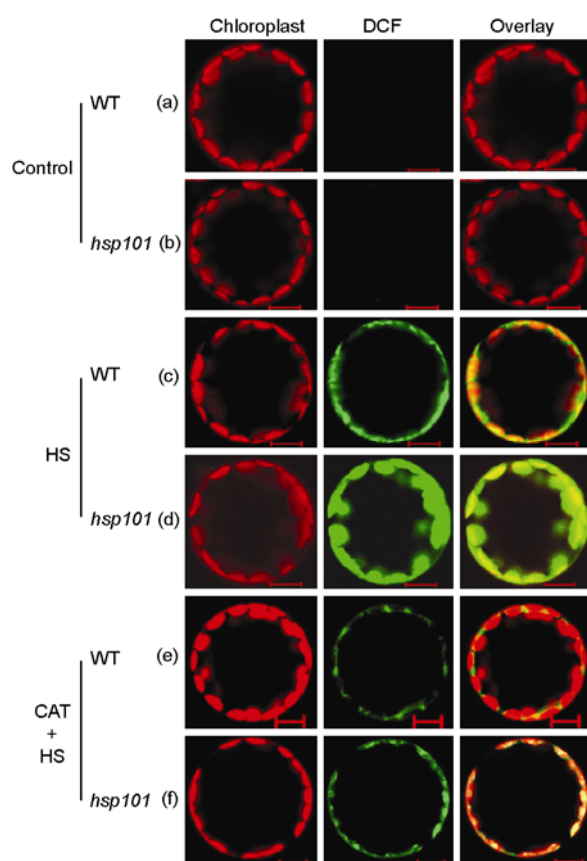


Figure 6 Intracellular ROS production and localization in the WT *Arabidopsis* and *hsp101* mutant protoplasts after HS. The protoplasts were pre-incubated without or with CAT at $100 \text{ U} \cdot \text{mL}^{-1}$ final concentration for 30 min in dark, and then left untreated or treated with HS. After 30 min of recovery, the samples were subjected to $5 \mu\text{M}$ H_2DCFDA for 10 min in dark, and the concentration of H_2O_2 was observed by the LCSM as described in “Material and method”. Scale bars = $10 \mu\text{m}$. This experiment was repeated three times with similar results.

hsp101 mutant protoplasts after 30 min of recovery following HS (Figure 6(c) and (d)). Obviously, the *hsp101* protoplasts displayed much stronger DCF fluorescence signal than the WT protoplasts (Figures 6(c) and (d)), which is consistent with the result obtained by the optical biosensor at leaf level (Figure 5(a)). In contrast, only little background of DCF signal could be detected in untreated protoplasts (Figure 6(a) and (b)). Furthermore, addition of CAT before HS dramatically depleted the DCF signals derived from chloroplasts in the WT *Arabidopsis* and *hsp101* mutant protoplasts (Figure 6(e) and (f)). The 3D reconstructed images produced from optical sections of cells showed that within the first 1 h of recovery following HS treatment, chloroplasts began to become round, and cell showed unwonted morphology in the WT protoplasts relative to the control protoplasts (Figure 7(a) and (c)). However, this abnormality was severer in the *hsp101* protoplasts after the same period of recovery (Figure 7(b) and (d)).

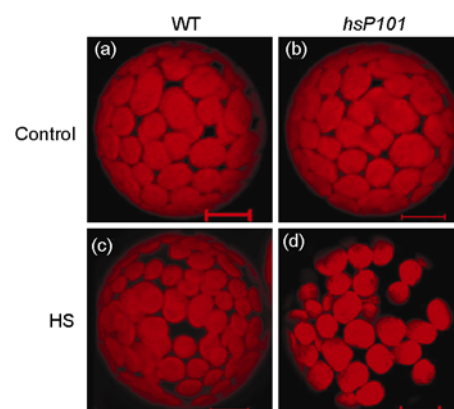


Figure 7 Changes in chloroplasts morphology after HS treatment. 3D reconstructed images were produced from optical sections of protoplasts which were left untreated or treated with HS. Note that after 1 h of recovery following HS (c and d), the *hsp101* protoplasts showed more chloroplasts with irregular stack and distribution in the cytoplasm than the WT protoplasts. Moreover, the chloroplasts of the *hsp101* protoplasts do not evenly reside near the plasma membrane compared with untreated cells or treated WT cells. The shape of the chloroplasts also become round (d). Scale bars = $10 \mu\text{m}$. This experiment was repeated three times with similar results.

3 Discussion

Contrastive measurements of DF intensity and Pn showed that the DF intensity correlated well with Pn in both the WT *Arabidopsis* and *hsp101* mutant plants after different temperature treatments (Figure 2). After HS, DF intensity and Pn responded to irradiance intensity in quite a consistent way (Figure 3), and showed a similar recovery dynamics in the WT *Arabidopsis* and *hsp101*

mutant plants, respectively (Figure 4). It is thus concluded that the proposed multi-parameter analyzing optical biosensor could be used to accurately assess the photosynthetic behavior under HS conditions.

DF intensity along with Pn consistently pointed out that the optimum temperature of photosynthesis for the *hsp101* mutant plants was far below that for the WT *Arabidopsis* (Figure 2). Photosynthetic performance indicated by both DF intensity and Pn was lower in the *hsp101* mutant than in the WT *Arabidopsis* at any given excitation light intensity (Figure 3). Moreover, after HS, the DF intensity and Pn both could fully recover in the WT *Arabidopsis* but not in the *hsp101* mutant plant (Figure 4). These results were in line with the observations obtained by other observers, who showed that Hsp101 was required for basal thermotolerance^[18,19].

The difference in thermotolerance between the WT *Arabidopsis* and *hsp101* mutant plants was also clearly reflected by using the new function of the optical biosensor to quantitatively detect ROS production *in vivo*. Within the first 30 min of recovery following HS, a higher level of ROS in the *hsp101* mutant plant than in the WT *Arabidopsis* could be seen regardless of the presence or absence of CAT (Figure 5), implying that the *hsp101* mutant might undergo severer oxidative damage than the WT *Arabidopsis* due to the absence of Hsp101, which was similar to the reports showing that the *hsp101* mutant produced a higher level of ROS than the WT plant after HS, and was more sensitive to oxidative stress^[18,19]. The conclusion was further strengthened by the results of single cell experiments, which showed more intensive DCF fluorescence at chloroplasts and severer abnormality of chloroplasts structure in the *hsp101* mutant than in the WT *Arabidopsis* protoplasts (Figures 6 and 7). Considering the results where ROS induced by HS were mainly localized at chloroplasts and addition of CAT could prevent the declines in DF inten-

sity in both the WT *Arabidopsis* and *hsp101* mutant plants (Figures 5 and 6), we thus speculated that the declines in photosynthetic performance might be attributed to the oxidative damages to photosynthetic apparatus.

To sum up, all testing results have demonstrated the effectiveness of the proposed optical biosensor for accurately monitoring HS responses and identifying the difference in thermotolerance between the WT *Arabidopsis* and *hsp101* mutant plants. This biosensor exploits the optical principle to detect photosynthetic performance, and thus it is different from commercially available equipment which is based on gas exchange technique. Therefore, this biosensor presented here was simplified, rapid, and in particular, was not prone to interference from environmental factors. Furthermore, the sensitivity of DF to environmental stresses, coupled with the ease that measurements of DF can be made by using the biosensor, makes the proposed optical biosensor potentially useful for non-invasive and real-time monitoring of plant stress responses. Moreover, the equipment of adjustable excitation source and its remote control mode make on-line, multi-parameter and *in vivo* inspection possible. In this regard, the proposed biosensor was extremely suitable for simultaneous analysis of photosynthetic behaviors and other stress responses such as ROS burst. In a word, the nature of new principle and one-machine multi-purpose might be important and useful for biotechnological and practical applications, although field testing and further improvements of the reported biosensor must be performed both for portable considerations and economical reasons.

We are grateful to Dr. Yee-yung Charng (Agricultural Biotechnology Research Center, Academia Sinica, Taipei, Taiwan) for kindly providing hsp101 mutants Arabidopsis seeds. We also thank Prof. Qun Chen and Dr. Li Jia for their help with language revision of the manuscript. We are greatly grateful to the anonymous reviewer for her insightful comments on the manuscript.

- 1 Hideg E, Barta C, Kalai T, et al. Detection of singlet oxygen and superoxide with fluorescent sensors in leaves under stress by photoinhibition or UV radiation. *Plant Cell Physiol*, 2002, 43: 1154–1164
- 2 Wang J S, Xing D, Zhang L R, et al. A new principle photosynthesis capacity biosensor based on quantitative measurement of delayed fluorescence *in vivo*. *Biosens Bioelectron*, 2007, 22: 2861–2868
- 3 Berry J, Björkman O. Photosynthetic response and adaptation to temperature in higher plants. *Annu Rev Plant Physiol*, 1980, 31: 491–543
- 4 Gratani L, Pesoli P, Crescente M F, et al. Photosynthesis as a temperature indicator in *Quercus ilex* L. *Glob Planet Change*, 2000, 24: 153–163
- 5 Vacca R A, Valenti D, Bobba A, et al. Cytochrome c is released in a reactive oxygen species-dependent manner and is degraded via caspase-like proteases in tobacco Bright-Yellow 2 cells en route to heat shock-induced cell death. *Plant Physiol*, 2006, 141: 208–219
- 6 Apel K, Hirt H. Reactive oxygen species: metabolism, oxidative stress, and signal transduction. *Annu Rev Plant Biol*, 2004, 55: 373–399
- 7 Genty B, Harbinson J, Baker N R. Relative quantum efficiencies of the two photosystems of leaves in photorespiratory and non-photo-

- respiratory conditions. *Plant Physiol Biochem*, 1989, 28: 1–10
- 8 Cheng L L, Fuchigami L H, Breen P J. The relationship between photosystem II efficiency and quantum yield for CO₂ assimilation is not affected by nitrogen content in apple leaves. *J Exp Bot*, 2001, 52: 1865–1872
 - 9 Murakami Y, Tsuyama M, Kobayashi Y, et al. Trienoic fatty acids and plant tolerance of high temperature. *Science*, 2000, 287: 476–479
 - 10 Yamasaki T, Yamakawa T, Yamane Y, et al. Temperature acclimation of photosynthesis and related changes in photosystem II electron transport in winter wheat. *Plant Physiol*, 2002, 128: 1087–1097
 - 11 Turzó K, Laczkó G, Filus Z, et al. Quinone-dependent delayed fluorescence from the reaction center of photosynthetic bacteria. *Biophys J*, 2000, 79: 14–25
 - 12 Li Q, Xing D, Jia L, et al. Mechanism study on the origin of delayed fluorescence by an analytic modeling of the electronic reflux for photosynthetic electron transport chain. *J Photochem Photobiol B*, 2007, 87: 183–190
 - 13 Wang C L, Xing D, Zeng L Z, et al. Effect of artificial acid rain and SO₂ on characteristics of delayed light emission. *Luminescence*, 2005, 20: 51–56
 - 14 Chaerle L, Van Der Straeten D. Seeing is believing: imaging to monitor plant health. *Biochim Biophys Acta*, 2001, 1519: 153–166
 - 15 Zhang L R, Xing D, Wang J S, et al. Rapid and non-invasive detection of plants senescence using a delayed fluorescence technique. *Photochem Photobiol Sci*, 2007, 6: 635–641
 - 16 Genty B, Briantais J M, Baker N R. The relationship between the quantum yield of photosynthetic electron transport and quenching of chlorophyll fluorescence. *Biochim Biophys Acta*, 1989, 990: 87–92
 - 17 Zhang L R, Xing D. Methyl jasmonate induces production of reactive oxygen species and alterations in mitochondrial dynamics that precede photosynthetic dysfunction and subsequent cell death. *Plant Cell Physiol*, 2008, 49: 1092–1111
 - 18 Rikhvanov E G, Gamburg K Z, Varakina N N, et al. Nuclear-mitochondrial cross-talk during heat shock in *Arabidopsis* cell culture. *Plant J*, 2007, 52: 763–778
 - 19 Charng Y Y, Liu H C, Liu N Y, et al. A heat-inducible transcription factor, HsfA2, is required for extension of acquired thermotolerance in *Arabidopsis*. *Plant Physiol*, 2007, 143: 251–262